Materials Chemistry and Physics 143 (2013) 60–64

Contents lists available at ScienceDirect

Materials Chemistry and Physics

journal homepage: www.elsevier.com/locate/matchemphys

Synthesis of porous micro-sized titania cages and their photocatalytic property

M.-C. Tsai [a,1], M.-H. Yang [a,1], Y.-W. Chang [a,1], J.-K. Tzeng [a,1], C.-Y. Lee [a,*], H.T. Chiu [b,2], H.-C. Chen [c], I.-N. Lin [c]

[a] Department of Materials Science and Engineering, National Tsing Hua University, Hsinchu 30034, Taiwan
[b] Department of Applied Chemistry, National Chiao Tung University, Hsinchu 30050, Taiwan
[c] Department of Physics, Tamkang University, New Taipei 25137, Taiwan

HIGHLIGHTS

- High surface area TiO_2 cubic cages were obtained by using NaF cubes as the template.
- TiO_2 formed on the {110} and {111} planes of a NaF cubes not on the {100} plane.
- Cage-like porous TiO_2 exhibited much greater photo-catalytic effectiveness.

GRAPHICAL ABSTRACT

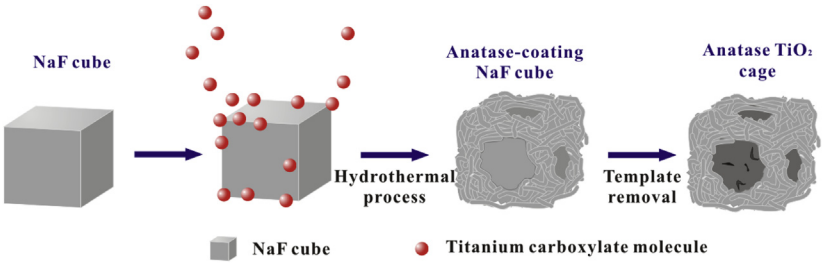

ARTICLE INFO

Article history:
Received 16 January 2012
Received in revised form
13 June 2013
Accepted 16 August 2013

Keywords:
Oxides
Sol–gel growth
Surface properties
Microstructure

ABSTRACT

Micro-sized TiO_2 cage consisted of anatase nanoparticles on the edges of each cube, was synthesized using TTIP as the reagent and NaF submicrometer sized cubes as the template. When a salt of cube was adopted as the template, the reactants prefer to grow on the active sites, edges and corners of the cube, after removing the NaF template, the skeleton of the cube remain as the cage-shaped materials. The hierarchical structures with nano-sized anatase particles and micro scaled cage architecture markedly enlarge the surface area and enhance the light harvesting by light scattering of TiO_2 frame, resulting in great photo-catalytic performance, which leads to the photo-degradation of methylene blue by 40% higher than that was achieved by crushed nanoparticles.

1. Introduction

TiO_2 has attracted considerable research attention owing to its extensive use in photo-catalysts [1–6], Li ion batteries [7,8], dye-sensitized solar cells (DSSC) [9–12], and bioassays [13]. Additionally, its non-toxicity, high chemical stability, ease of synthesis and, in particular, its superior characteristics towards the nanometer-scale have made TiO_2 increasingly important. Owing to the listed properties, researchers in environmental science favor TiO_2, especially for the photo-degradation of organic pollutants, also known as photocatalysts. Despite these advantages, the performance of the TiO_2 photocatalysts is strongly affected by its structure, heterogeneous interface, size and exposed faces in solution [14–16]. In recent years, the hierarchical mesoporous structure of TiO_2 has been extensively studied in DSSC and photocatalysis applications and showed significantly improved performance [17–21]. Hierarchical

* Corresponding author. Fax: +886 3 5166687.
E-mail addresses: cylee@mx.nthu.edu.tw (C.-Y. Lee), htchiu@cc.nctu.edu.tw (H.T. Chiu), inanlin@mail.tku.edu.tw (I.-N. Lin).
[1] Fax: +886 3 5166687.
[2] Fax: +886 3 5723764.

0254-0584/$ – see front matter © 2013 Elsevier B.V. All rights reserved.
http://dx.doi.org/10.1016/j.matchemphys.2013.08.011

Table 1
The post-treatment conditions, structure characterization and photo-degradation rate constant for all samples.

Sample	Post-treatment parameters						
	HCl treatment	Anneal (temp. time)	Composition	Structure	Morphology	Grain size[a] (nm)	k (min^{-1})
PC	–	–	Na, F, Ti, O	Mixed phases	Cage		
AC	8 h	–	Ti, O	Anatase	Cage	4.0	0.003
AC550	8 h	450 °C, 2 h 550 °C, 2 h	Ti, O	Anatase	Cage	13.8	0.039
ANP550	–	550 °C, 4 h	Ti, O	Anatase	Particle	24.1	0.019
5 nm[b]	–	–	Ti, O	Anatase	Particle		0.012
RDH[c]	–	–	Ti, O	Anatase	Particle		0.024

[a] Data from XRD.
[b] Nano-sized TiO_2.
[c] Micro-sized TiO_2.

structure takes the advantage of macron architecture, such as hollow spherical or channel-like structures, and high surface area frame structures to improve the light harvest and reaction activity. When light enters one of these unique architectures, it would be trapped by reflection and scattering, increasing the interaction between the light and the TiO_2 [22,23]. Moreover, the porous frame of hierarchical structure possesses of the high surface area enhanced reaction activity. There are several types of hierarchical structure materials, such as nanotube arrays, urchin-like materials, mesoporous spheres and hollow spheres, have been reported and studied widely [17,18,22,23]. Among these hierarchical structures, mesoporous spheres and hollow spheres attracted the most attentions in the fields of power generation and environment. Caruso et al. prepared an electrode using TiO_2 mesoporous spheres synthesized by the hydrothermal method for DSSC application [11]. Scattering between the particles markedly elongates the travel path of light in the electrode, increasing the light utilization, which leads to significantly improved the performance of DSSC. Furthermore, Yang et al. prepared uniform TiO_2 hollow spheres by a self-templating method and systematically studied the factors affecting photocatalytic activities [14]. However, to the best of the authors' knowledge, cubic mesoporous cages have been seldom reported so far despite that many kinds of hierarchical structures have been investigated in detail.

Herein, mesoporous cage-like particles with high surface area were prepared by a template method, in which titanium oxide selectively grew on the cubic NaF submicro template. The corners and edges of NaF cubes, with high surface energy, act as preferential nucleating site for TiO_2 nanoparticles growing on to yield the hierarchical TiO_2 cubic cages. Moreover, the hierarchical cage TiO_2 was used as a highly efficient photocatalyst.

2. Experimental section

2.1. Preparation of nanocages

All chemicals in this work were purchased from the Aldrich Company and used directly without any pretreatment. The procedure for synthesizing anatase nanocages was described as follows. Firstly, a solution containing well-dispersed NaF seeds was prepared by mixing NaF water solution (0.5 M, 6 mL) with ethanol (24 mL). Secondly, a precursor solution containing titanium source was prepared by mixing titanium isopropoxide (0.3 mL) and valeric acid (1.2 mL) in ethanol (50 mL) solution, and followed by a reflux at 85 °C for 6 h. After the reflux, the NaF seed solution was added into the precursor solution and kept reflux for a further 3 h to initiate hydrolysis and condensation reaction. The powder, which has a cage-like shape, was collected by a centrifuge and washed by DI water several times to remove NaF seeds. The sample of pristine cages then dried at 50 °C and named PC in convenience. Pristine cage was further treated with HCl solution (pH 3) for 8 h to removed impurity phase and the residual was washed by DI water until the solution was neutral. After HCl treatment, pure anatase phase cages were obtained and denoted as AC. The AC sample was annealed at 450 °C for 2 h followed by annealing of 550 °C for 2 h in order to improve crystallinity. The final product was marked as AC550. In order to elucidate the effect of cage shape on photocatalytic test, TiO_2 nanoparticles were also prepared by annealing at 550 °C for 4 h without acid treatment, which was marked as ANP. Table 1 lists the conditions for all samples and morphologies of all final products.

2.2. Characterization

The morphology and composition of the samples were studied using a JEOL-6500 FE-SEM that was equipped with an EDS (energy dispersive spectrometer). Transmission electron microscope (TEM) images were obtained using a JEOL-2010 TEM with an accelerating voltage of 200 keV. The structure of the samples was identified using an X-ray diffraction (XRD) meter (Brucker D8-advanced) with Cu Kα radiation ($\lambda = 0.154$ nm). The mean crystallite size of anatase grains was calculated using the Scherrer formula ($d = 0.9\,\lambda/B\cos\theta$), where d, λ, B and θ are crystallite size, Cu Kα wavelength (0.154 nm), full width at half maximum intensity (FWHM) of the (1 0 1) anatase peak in radians, and Bragg's diffraction angle, respectively.

2.3. Measurement of photocatalytic activity

The light source was a 150 W Xe bulb from Osram, and the temperature was maintained at 296 K by a water cooling system. 0.01 g TiO_2 powder was mixed completely with 70 mL of DI water and 10 mL of 0.625 mM methylene blue solution, which acted as a target pollutant. The solution was illuminated from the top while being stirred using a magnetic stirrer. Samples were extracted every 5 min, and after they were filtered through a 0.2 μm filter, all of the samples were diluted with 1.5 mL DI water. The target pollutant concentration was studied using a UV–Vis spectroscope.

3. Results and discussion

A micrometer sized cage-like TiO_2 which is composed of anatase nano-sized particles were synthesized by refluxing a mixture of TTIP and valeric acid in an aqueous solution with NaF cube particles as the template, followed by heat and acid treatments. The reaction conditions and powder properties are summarized in Table 1. Fig. 1 presents SEM images of 200 nm edge length NaF template and powders of TiO_2 cages before and after different post-treatments. The pristine cage-like product, PC, with about 1 μm edge length consist of the aggregation of 200 nm sized particles, were obtained after removal of NaF templates. The energy dispersive X-ray spectrum (EDS) in the inset of Fig. 1b indicates the presence of F, Na, Ti and O in the powders, showing that an insoluble impurity phase

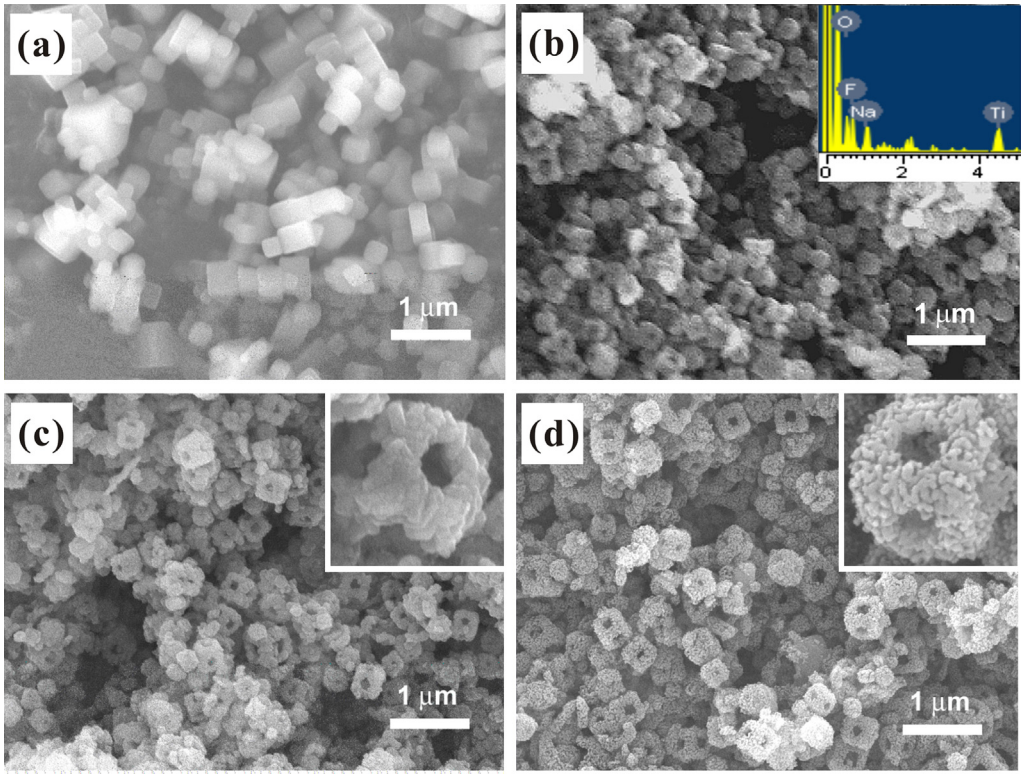

Fig. 1. SEM images of (a) NaF cubes. (b) Cages before acid treatment (PC). (c) The PC sample after acid treatment (AC). (d) The AC sample after annealing (AC550).

formed during the reaction. According to XRD analysis shown in Fig. 2, the impurity phase in the PC has a layered structure in lattice according to a diffraction peak at small 2θ angle, 15°, which is usually featured by metal titanates [24,25]. To obtain pure anatase TiO_2 cage, PC was immersed in HCl solution for 8 h to remove the impurity that contains fluorine and sodium, the yielded powder was designated as AC. After acid wash, only anatase phase was left in the final product, which was evidenced by the existing X-ray diffraction peaks in Fig. 2 which could be assigned to TiO_2 anatase phase according to JCPDF card (89-4921). At the end of the sample preparation for photocatalytic test, two different ways of heat treatments were applied to improve AC crystallinity. One of the AC samples was annealed at 550 °C directly for 4 h and the other sample was annealed at 450 °C for 2 h, and then at 550 °C for 2 h, two samples were designated as ANP550 and AC550, respectively. The XRD patterns of both samples are also included in Fig. 2 with other samples for comparison. Upon calcination at 550 °C, the peaks of the annealed powders reveal better crystallinity for both AC550 and ANP550 than without calcination. Although, calcination improved the crystallinity of TiO_2 anatase cages, ramp rate of heat treatment greatly affect the morphology of final products. The morphology of ANP550 no longer kept under high ramping rate, turning into particulate shape, whereas for AC550, the frame was transformed to a worm-like mesoporous structure while preserving cage shape. Moreover, the grain sizes, estimated by Scherrer equation, were 4.0, 24.1, and 13.8 nm for AC, ANP550, and AC550, respectively. These observations reveal that the powder synthesized by TTIP and NaF followed by acid treatment and annealing is a macro sized cage-like powder that comprises nano-sized anatase TiO_2.

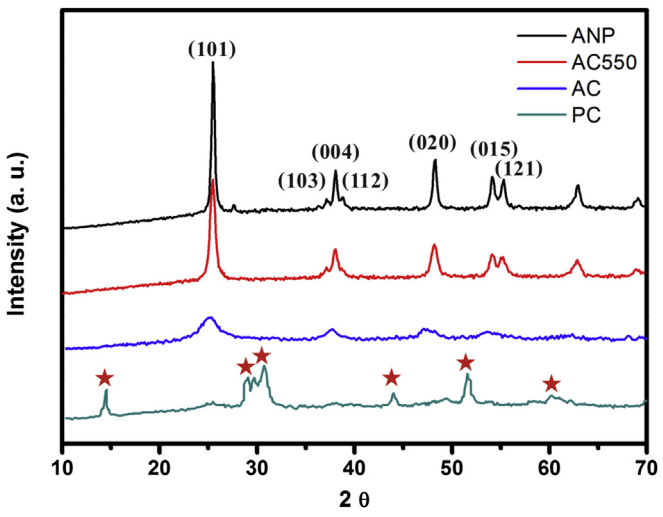

Fig. 2. X-ray diffraction patterns (XRD) of porous cubic cages TiO_2 before and after different post-treatments.

TiO_2 cages before and after annealing were examined by TEM, as displayed in Fig. 3. The TEM images demonstrate that the internal space that is defined by the cage's edges is empty and the larger particles of the AC powder with a size of approximately 50 nm shrink to about 10 nm upon heating (AC550). The SAED study of the annealed powder yields a diffused-ring pattern, suggesting that its structure is polycrystalline. The ED rings can be indexed to the (101), (004), (200), and (105) planes of anatase TiO_2, that is corresponding to the observation from XRD analysis (Fig. 2). Fig. 3d shows a HRTEM image of annealed powder. The grains have an average diameter of 10 nm. Also, the lattice fringes with a spacing of 0.35 nm can be assigned to the (101) planes of anatase TiO_2 as well.

Herein, a growth pathway of the cubic cages is proposed. As we know, the morphology of the materials can be tuned by templates such as surfactants and the preferential growth direction [26–28]. With respect to crystal growth, the morphology of particles is basically determined by the ratio of the growth rate in the [1 0 0]

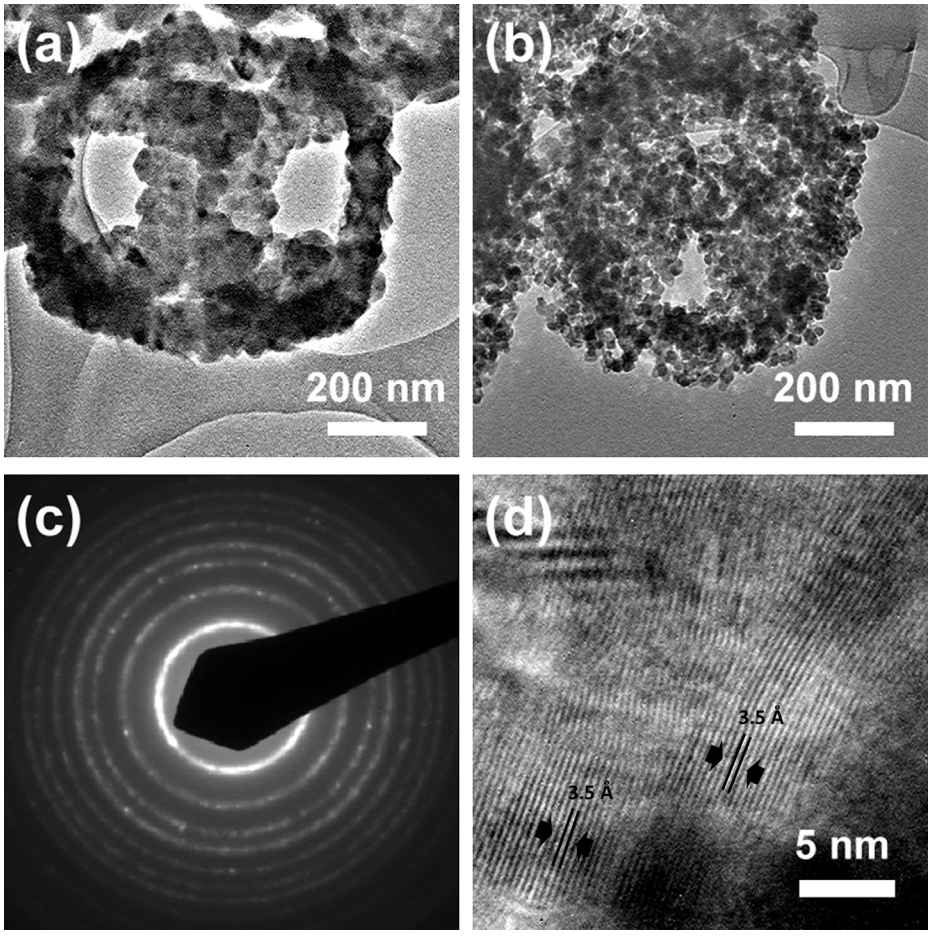

Fig. 3. TEM analysis of porous cubic TiO_2 cages; (a) before annealing (AC). (b) After annealing (AC550). (c) and (d) SAED pattern and HRTEM image of AC550.

direction to that in the [1 1 1] direction. When the growth on the [1 1 1] face is much faster than that on the [1 0 0] face, cubes are obtained. Otherwise, spherical crystals were obtained. The formation of spheres is well known to be preferred in a homogeneous solution as it minimizes the surface energy, while heterogeneous growth is preferred in the presence of a seed in a solution [29]. In this work, NaF nanocrystal was used as a sacrificial template. Therefore, TiO_2 nanoclusters were heterogeneously grown on {111} and {110} planes, especially on the edges of NaF nanocrystal with high surface energy, to form a cage-like material instead of spherical solid.

Fig. 5 presents the photocatalytic behaviors of AC, AC550 and ANP550 in the degradation of methylene blue (MB) under irradiation by UV light. Commercial anastase TiO_2 micro-sized about 100–300 nm diameter and nano-sized with a 5 nm diameter were also tested for comparison. The materials characterizations including SEM, TEM images and XRD of commercial TiO_2 are shown in Fig. 4. The MB concentration decays by around 50% when sample micro-size TiO_2 or ANP550 is adopted and by approximately 68% when AC550 is used. As AC was used as the photocatalyst, the concentration decay of MB is only around 15%, whereas nano-sized TiO_2 show 30% concentration decay of methylene blue. For a convenient comparison, the rate constant (k) was adopted to evaluate the performance of TiO_2 photocatalysts. The reaction of MB degradation was a first-order reaction, and a straight line was obtained when logarithmic concentration was plotted against time, $k = -[\ln(C/C_0)]/\Delta t$, where C is the concentration; C_0 is the initial concentration; Δt is the time passed and k is the pseudo-first-order rate constant. Table 1 includes the rate constant, k, for all TiO_2 photocatalysts in this work.

Among these photocatalysts, AC550 has the best photocatalytic performance for the degradation of MB. There are several factors that greatly affect photocatalytic activity such as surface area, exposed crystalline faces, heterojunctions [14]. Herein, in order to clarify the enhancement factor for AC550, discussion based on two factors, crystallinity and hierarchical structure of TiO_2 photocatalysts is made. Regarding crystallinity, we choose AC, AC550 and ANP550 for comparison. Both ANP550 and AC550, which were post-annealed and exhibited a good crystallinity, have a huge improvement of photocatalytic activity over AC which was only acid-treated. Moreover, two TiO_2 photocatalysts with fair good crystallinity, AC550, ANP550 were chosen for clarifying the effect of hierarchical structure. AC550 still has the best photocatalytic activity between these photocatalysts due to taking advantage of its mesoporous cage-like hierarchical structure with high surface area. It was reported that special hierarchical structured materials keep micron-scale inherent properties that could harvest light more by the scattering effect in micron structure where resonance effect in light-scattering emerges as the size of the particle approaches the wavelength of incident light [14,22,23]. The rate constant of AC550 over ANP550 gave a strong evidence for the enhancement of photocatalytic activity by hollow cage-like structure. We also compared anatase nanocages AC550 to two commercial TiO_2, micro-sized TiO_2 and nano-sized TiO_2. In this part, AC550 still performs excellent due to its comprehensive property. Surprisingly, photocatalytic activity of nano-sized TiO_2 is inferior to that of micro-sized TiO_2

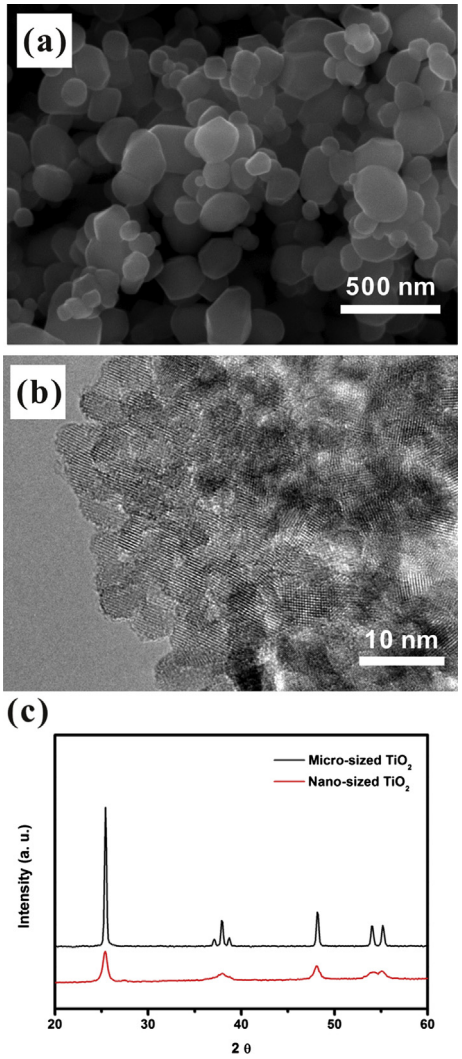

Fig. 4. Characterizations of commercial TiO_2 particles (a) SEM image of the micro-sized TiO_2 with 100–300 nm in size. (b) TEM image of nano-sized TiO_2 with 5 nm. (c) X-ray diffraction patterns (XRD) of both commercial TiO_2 particles used in this work.

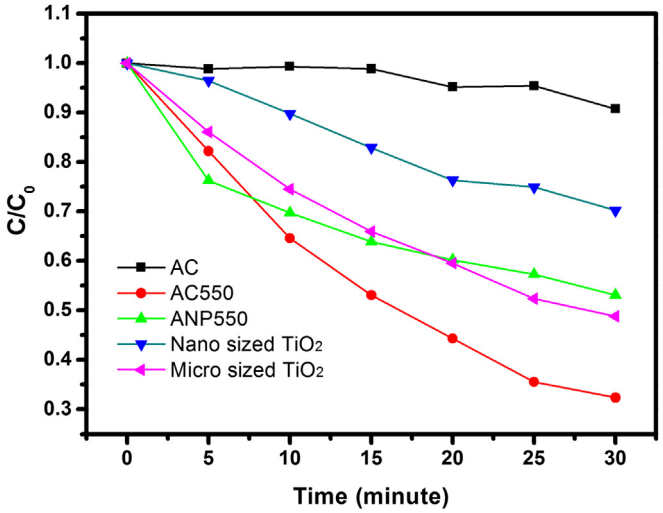

Fig. 5. Photocatalytic performance of TiO_2 cubic cages after different post-treatments (AC, AC550, ANP550) and commercial TiO_2 used in this work (nano-sized and micro-sized TiO_2).

even though nano-sized TiO_2 has larger surface area due to its smaller particle size. This strongly supports the result that the photocatalysts possessing better crystallinity have higher photo-catalytic activity even with smaller surface area, which was shown in previous discussion on AC and ANP550. Based on the discussion above, the morphology and the crystallinity of the powder markedly affected its photo-catalytic activity.

4. Conclusions

Highly dispersed TiO_2 nanocages were synthesized by a sol–gel process in which TTIP was hydrolyzed to form TiO_2 on the {110} and {111} planes rather than on the {100} plane of a NaF cubic template. Owing to the good crystallinity and hierarchical structure with effective light harvesting property and large surface area, cage-like porous TiO_2 exhibited superior photo-catalytic effectiveness to that of other micro- and nano-scaled TiO_2 particles.

Acknowledgment

The authors would like to thank the National Science Council of the Republic of China, Taiwan, for financially supporting this research under contract no. NSC 101-2113-M-007-012-MY3 and NSC 101-2811-M-032-013.

References

[1] C.-W. Peng, T.-Y. Ke, L. Brohan, M. Richard-Plouet, J.-C. Huang, E. Puzenat, H.-T. Chiu, C.-Y. Lee, Chem. Mater. 20 (2008) 2426.
[2] H.A. Chen, S. Chen, X. Quan, Y.B. Zhang, Environ. Sci. Technol. 44 (2010) 451.
[3] T.A. Kandiel, A. Feldhoff, L. Robben, R. Dillert, D.W. Bahnemann, Chem. Mater. 22 (2010) 2050.
[4] S.W. Liu, J.G. Yu, M. Jaroniec, J. Am. Chem. Soc. 132 (2010) 11914.
[5] S.W. Liu, J.G. Yu, S. Mann, Nanotechnology 20 (2009).
[6] J. Zhang, Z.P. Zhu, Y.P. Tang, X.L. Feng, J. Mater. Chem. A 1 (2013) 3752.
[7] M.-C. Tsai, J.-C. Chang, H.-S. Sheu, H.-T. Chiu, C.-Y. Lee, Chem. Mater. 21 (2009) 499.
[8] P.C. Chen, M.C. Tsai, H.C. Chen, I.N. Lin, H.S. Sheu, Y.S. Lin, J.G. Duh, H.T. Chiu, C.Y. Lee, J. Mater. Chem. 22 (2012) 5349.
[9] F. Zhu, D.P. Wu, Q. Li, H. Dong, J.M. Li, K. Jiang, D.S. Xu, RSC Adv. 2 (2012) 11629.
[10] H.Y. Chen, D.B. Kuang, C.Y. Su, J. Mater. Chem. 22 (2012) 15475.
[11] D.H. Chen, F.Z. Huang, Y.B. Cheng, R.A. Caruso, Adv. Mater. 21 (2009) 2206.
[12] Y.J. Kim, M.H. Lee, H.J. Kim, G. Lim, Y.S. Choi, N.G. Park, K. Kim, W.I. Lee, Adv. Mater. 21 (2009) 3668.
[13] M.-C. Tsai, T.-L. Tsai, D.-B. Shieh, H.-T. Chiu, C.-Y. Lee, Anal. Chem. 81 (2009) 7590.
[14] M.-H. Yang, M.-C. Tsai, Y.-W. Chang, Y.-C. Chang, H.-T. Chiu, C.-Y. Lee, Chem. Cat. Chem. 5 (2013) 1871.
[15] H.G. Yang, C.H. Sun, S.Z. Qiao, J. Zou, G. Liu, S.C. Smith, H.M. Cheng, G.Q. Lu, Nature 453 (2008) 638.
[16] T.Y. Ke, C.Y. Lee, H.T. Chiu, Appl. Catal. A – Gen. 381 (2010) 109.
[17] J.Y. Liao, B.X. Lei, D.B. Kuang, C.Y. Su, Energy Environ. Sci. 4 (2011) 4079.
[18] K.Y. Yan, Y.C. Qiu, W. Chen, M. Zhang, S.H. Yang, Energy Environ. Sci. 4 (2011) 2168.
[19] P.C. Chen, M.C. Tsai, M.H. Yang, T.T. Chen, H.C. Chen, I.C. Chang, Y.C. Chang, Y.L. Chen, I.N. Lin, H.T. Chiu, C.Y. Lee, http://dx.doi.org/10.1016/j.apcatb.2013.1005.1076.
[20] J.G. Yu, Y.R. Su, B. Cheng, Adv. Funct. Mater. 17 (2007) 1984.
[21] J.G. Yu, W. Liu, H.G. Yu, Cryst. Growth Des. 8 (2008) 931.
[22] K. Zhu, N.R. Neale, A. Miedaner, A.J. Frank, Nano Lett. 7 (2007) 69.
[23] H.X. Li, Z.F. Bian, J. Zhu, D.Q. Zhang, G.S. Li, Y.N. Huo, H. Li, Y.F. Lu, J. Am. Chem. Soc. 129 (2007) 8406.
[24] T. Sasaki, M. Watanabe, Y. Fujiki, Y. Kitami, Chem. Mater. 6 (1994) 1749.
[25] D.V. Bavykin, J.M. Friedrich, F.C. Walsh, Adv. Mater. 18 (2006) 2807.
[26] T.K. Huang, T.H. Cheng, M.Y. Yen, W.H. Hsiao, L.S. Wang, F.R. Chen, J.J. Kai, C.Y. Lee, H.T. Chiu, Langmuir 23 (2007) 5722.
[27] P.C. Chen, M.C. Tsai, Y.J. Huang, H.T. Chiu, C.Y. Lee, Crystengcomm 14 (2012) 1990.
[28] M.H. Yang, P.C. Chen, M.C. Tsai, T.T. Chen, I.C. Chang, H.T. Chiu, C.Y. Lee, Crystengcomm 15 (2013) 2966.
[29] R. Buonsanti, V. Grillo, E. Carlino, C. Giannini, M.L. Curri, C. Innocenti, C. Sangregorio, K. Achterhold, F.G. Parak, A. Agostiano, P.D. Cozzoli, J. Am. Chem. Soc. 128 (2006) 16953.